Computational Modeling of Astrocyte Endfeet: Insights into their Mechanical Buffering Function

Marius Causemann*, Rune Enger† & Marie E. Rognes*

*Dept. of Numerical Analysis and Scientific Computing, Simula Research Laboratory

†Dept. of Basic Medical Sciences, University of Oslo

*mariusca@simula.no

The physiological role of astrocyte endfeet during vasodilation

Astrocyte endfeet encompass cerebral blood vessels, forming a nearly complete sheet, yet their functional significance remains incompletely understood. Current hypotheses include facilitating solute clearance [1] and regulating arteriole vasodilation and vasoconstriction. Furthermore, the abundance of Aquaporin-4 (AQP4) water channels on the endfoot side facing blood vessels raises questions about their physiological function. Recent imaging studies have demonstrated significant endfoot deformations during pronounced vasomotion during sleep [2], suggesting a potential mechanical buffering function that mitigates the mechanical forces exerted on the surrounding brain tissue.

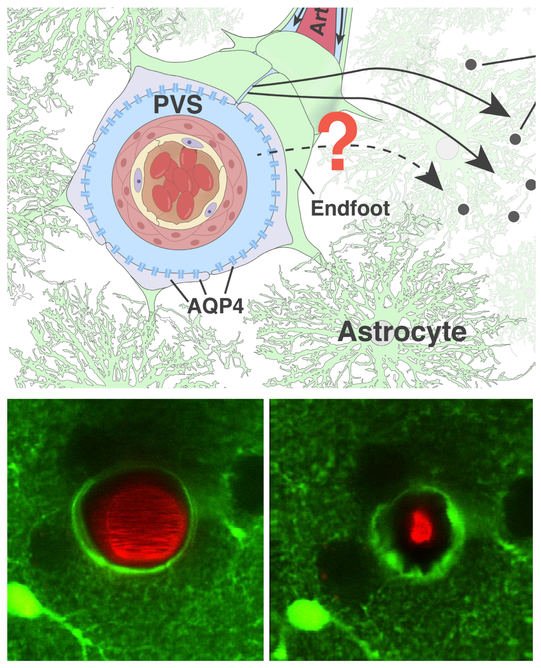

Figure 1: Astrocyte endfeet enwrap cerebral blood vessels and limit the perivascular space (PVS); endfeet (green) undergo substantial mechanical deformations during vascular (red) dilation [3]

Meshing the glia-vascular interface based on electron microscopy data

Challenge

- many intricate structures & details
- reduced extracellular space (ECS) due to chemical fixation

Meshing pipeline

- preprocess image on voxel level
- generate multidomain mesh from extracted surfaces

Reconstructed glia-vascular geometry

- length: 20 µm, vessel diameter: 10 µm
- domain includes PVS, ECS and five astrocyte endfeet

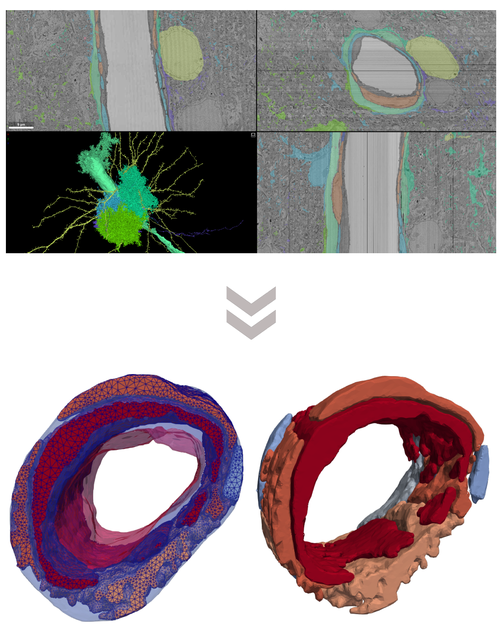

Modelling the mechanics of glia-vascular coupling

We model the intracellular space Ω_i (the astrocyte endfeet) and the extracellular space Ω_e (the PVS and ECS between the endfeet) as porous media consisting of an elastic solid matrix (cytoskeleton, extracellular matrix) filled with intra- and extracellular fluid. The permeable cell membrane Γ separates both domains and allows pressure-driven fluid exchange.

The evolution of pressure p and displacement $\mathbf{d}$ in space and time can be described by the equations of **Linear Poroelasticity**

$$-\mathbf{div}[2\mu_S\epsilon(\mathbf{d}) + \lambda \operatorname{div} \mathbf{d} - \alpha p\mathbf{I}] = 0 \quad \text{in } \Omega_i \cup \Omega_e \tag{1}$$

$$s\partial_t p - \alpha\partial_t \operatorname{div} \mathbf{d} + \operatorname{div}\left(\frac{\kappa}{\mu_F}\nabla p\right) = 0 \quad \text{in } \Omega_i \cup \Omega_e \tag{2}$$

with a Robin-type interface condition for the pressure-driven transmembrane fluid flux $\mathbf{q} = -\frac{\kappa}{\mu_F}\nabla p$:

$$\mathbf{q}\cdot\mathbf{n} = L_p[\![p]\!] \quad \text{on } \Gamma \tag{3}$$

Further, we impose mass conservation, displacement continuity and momentum conservation on the cell membrane:

$$[\![\mathbf{q}\cdot\mathbf{n}]\!] = 0; \quad [\![\mathbf{d}]\!] = 0; \quad [\![(2\mu_S\epsilon(\mathbf{d}) + \lambda \operatorname{div} \mathbf{d} - \alpha p\mathbf{I})\cdot\mathbf{n}]\!] = 0 \text{ on } \Gamma \tag{4}$$

The model is parameterized by the Lamé constants μ_S and λ, the Biot-Willis coefficient α, the storage coefficient s, the permeability κ, the fluid viscosity μ_F and the hydraulic conductivity of the cell membrane L_p.

We prescribe a sinusoidal expansion of the blood vessel wall as a driver of motion and simulate three cardiac cycles (0.3 s).

Vascular expansion drives PVS compression and endfoot sheath dilation

Investigating cardiac-driven small amplitude vessel oscillations (50 nm), we observe a reduction in PVS width and increased mechanical stress on the endfoot sheath during vessel expansion.

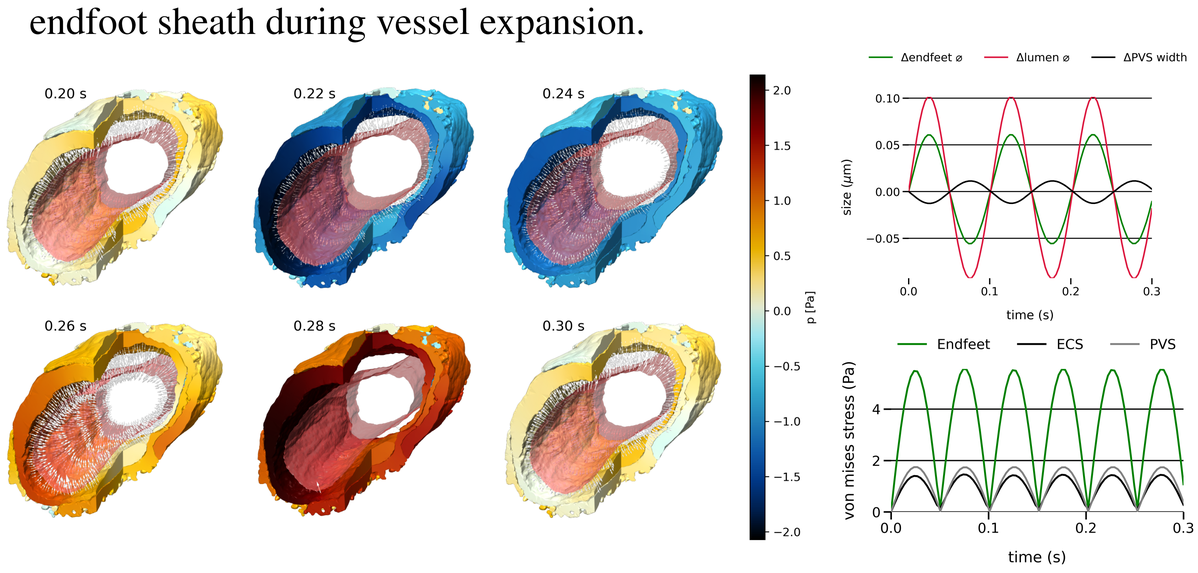

Figure 2: Intracellular pressure and PVS flow (arrows) (left); endfeet and lumen diameter and PVS width (top right); mean von Mises stress in endfeet, ECS and PVS (bottom right)

Intra- and extracellular fluid pressure evolve inversely

The dilation of the vascular wall raises the extracellular pressure, whereas the intracellular pressure decreases due to the volume increase of the dilated endfeet. Accordingly, we observe opposing fluid flow directions across the model's outer boundary.

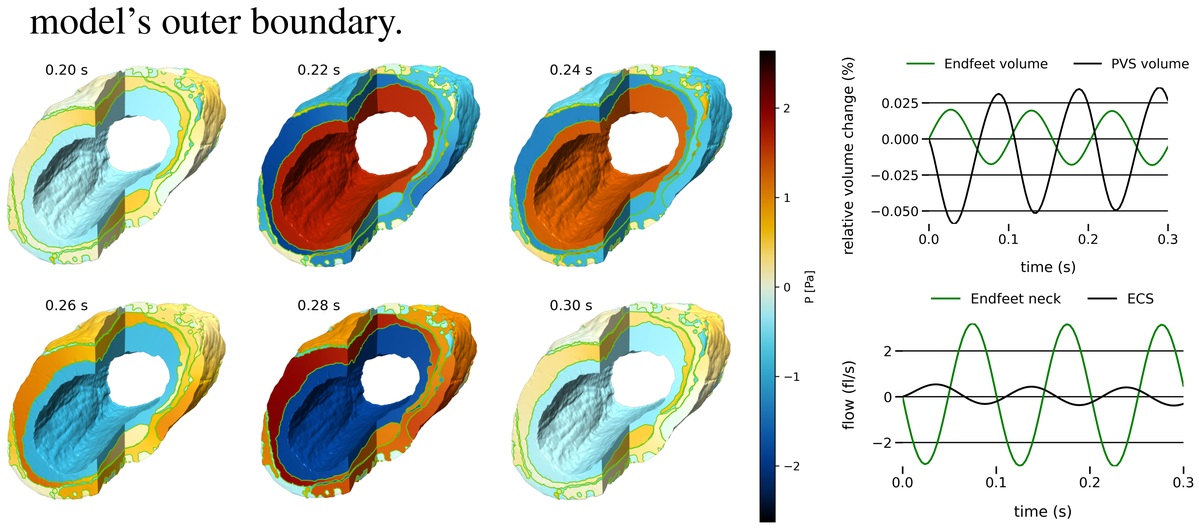

Figure 3: Intracellular and extracellular pressure over one cardiac cycle (left); volume change of endfeet and PVS (top right); flow across the model boundary (bottom right)

AQP4 has a negligible effect on glia-vascular mechanics

Comparing a wild-type and an AQP4 knock-out model (sevenfold reduction in membrane hydraulic conductivity) and computing key metrics of glia-vascular mechanics reveals only minor differences between both models.

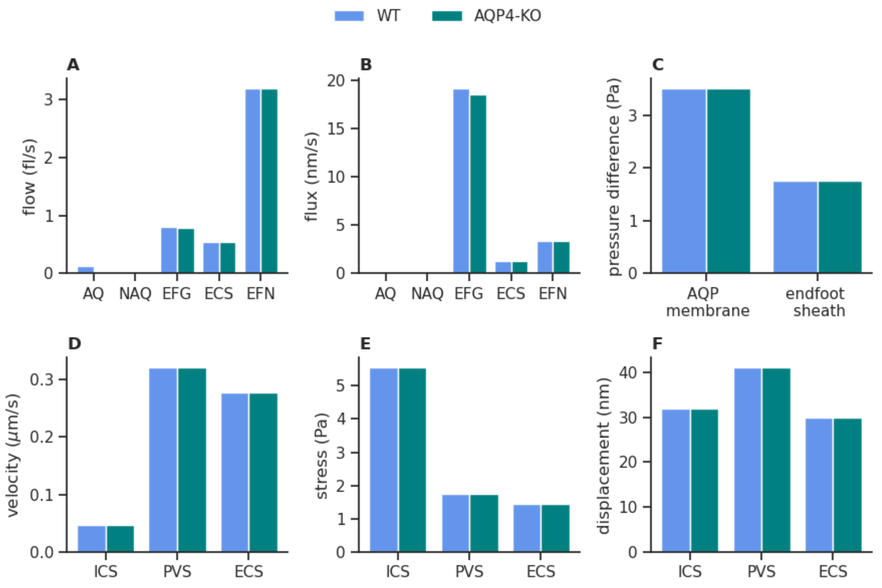

Figure 4: Glia-vascular mechanics of wild-type (WT) and AQP4 knockout (AQP4-KO) mice (AQ and NAQ - AQP4 dense and sparse membrane sections, EFG - endfeet gaps, EFN - endfeet neck, outer boundary of the endfeet)

References

[1] N. J. Abbott, M. E. Pizzo, J. E. Preston, D. Janigro, and R. G. Thorne. The role of brain barriers in fluid movement in the cns: is there a 'glymphatic'system? *Acta neuropathologica*, 135:387–407, 2018.

[2] L. Bojarskaite, A. Vallet, D. M. Bjørnstad, K. M. Gullestad Binder, C. Cunen, K. Heuser, M. Kuchta, K.-A. Mardal, and R. Enger. Sleep cycle-dependent vascular dynamics in male mice and the predicted effects on perivascular cerebrospinal fluid flow and solute transport. *Nature communications*, 14(1):953, 2023.

[3] A. B. Rosic, D. B. Dukefoss, K. S. Åbjørsbråten, W. Tang, V. Jensen, O. P. Ottersen, R. Enger, and E. A. Nagelhus. Aquaporin-4-independent volume dynamics of astroglial endfeet during cortical spreading depression. *Glia*, 67(6):1113–1121, 2019.

MC and MR acknowledge support from the Research Council of Norway via FRIPRO grant 324239 (EMIx) and from the national infrastructure for computational science in Norway, Sigma2, via grant NN8049K.